IOP Conf. Series: Journal of Physics: Conf. Series **852** (2017) 012002 doi:10.1088/1742-6596/852/1/012002

Limiting magnitudes and night sky brightness at the Langkawi National Observatory based on observations of standard stars

C -C Ngeow and S -C Luo

Graduate Institute of Astronomy, National Central University, Jhongli 32001, Taiwan

E-mail: cngeow@astro.ncu.edu.tw

Abstract. We present the estimation of limiting magnitudes and night sky brightness at the Langkawi National Observatory with observations of selected standard stars. We first derived the transformation equations using the standard stars in our CCD images, followed by photometric calibration of the 2MASS point sources located in these images. Based on the calibrated magnitudes, we estimated a limiting magnitude of V=16.6±0.1 mag can be reached with a 60 second exposure time. For the night sky brightness, our measurements give V_{sky}=19.0±0.1 mag arc-second^{-2} at the zenith direction. Our results can be used for planning the night time observations at the Langkawi National Observatory.

1. Introduction

The Langkawi National Observatory (hereafter LNO) is one of the research facility under the administration of ANGKASA (the Malaysian National Space Agency). Being located near the equator, LNO has an advantage to observe both of the northern and southern sky. LNO hosted several small-aperture telescopes, among them the 20-inch Ritchey-Chretien (RC) reflector telescope is the main telescope used for night time observations. This telescope has a focal length of 4115mm and hence a focal ratio of f/8.1, housing inside a 5m ObservaDOME. This telescope uses a Paramount-ME German equatorial mount for pointing and tracking celestial objects. A SBIG 1001E CCD Camera is equipped on the telescope. This CCD has 1024×1024 pixels, each pixels has a size of$24\mu m \times 24\mu m$, which produces a field-of-view of $20.1' \times 20.1'$ with a pixel scale of 1.2" per pixel. According to the vendor, this CCD can reach to quantum efficiency (Q.E.) of ~75% at 5500Å. The CCD has a gain of 2.2e^-/ADU and a typical readout noise of 15e^- RMS. Data taken from the LNO's telescope and CCD has been used in the study of, for example, the transit of a exoplanet HAT-P-13 [1]. In addition to CCD imaging, this 20-inch RC telescope has also been used in spectroscopic observations [2, 3, 4]. Recently, LNO has acquired an observatory code as O43 from the Minor Planet Center [5].

Both of the limiting magnitudes and night sky brightness are two important metrics to evaluate the observing capability of an observatory, as well as for the planning of night time imaging observations. For example, a celestial object with an apparent magnitude fainter than the limiting magnitude is impossible to be observed. A limiting magnitude of V=18.6±1.0 mag, inferred from the night sky brightness, has been measured at LNO in the past [6]. However, this measurement was done using a different combination of the telescope and detector – the Meade LX200GPS 8-inch Schmidt-Cassegrain telescope and a SBIG STV camera. Therefore, it is important to measure the limiting magnitudes and night sky brightness at LNO directly from the 20-inch RC telescope and the SBIG

1001E CCD mentioned above. In this work, we present such measurements based on the observations of selected standard stars at the LNO. The observations were described in Section 2, followed by Section 3 on data reduction and analysis. In Section 4 we present our estimation of the limiting magnitudes and night sky brightness at LNO. A conclusion of this work is given in Section 5.

2. Observations

Our observation of standard stars at LNO was carried out on the night of 01 April, 2016. The night was clear and appeared to be photometric. The third quarter Moon was illuminated by ~45%, and rose around 01:44am local time. A number of standard stars were selected from [7], and they were observed at various air masses with standard broad-band BVRI filters. Our selected standard stars and the corresponding standard stars fields are:

- GD 108: GD 108, GD 108A, GD 108B, GD 108C, GD 108D
- SA104: SA104 350, SA104 364, SA104 456, SA104 457, SA104 460, SA104 461, SA104 470
- PG0918: PG0918+029, PG0918+029A, PG0918+029B, PG0918+029C, PG0918+029D
- PG1323: PG1323-086, PG1323-086A, PG1323-086B, PG1323-086C, PG1323-086D

Table 1 gives the list of observed standard stars fields and the observing log. In total, 48 images were acquired in BVRI filters for the selected standard stars in four different standard star fields.

Table 1. Observing Log for Standard Stars Observations at LNO on 01 April 2016.

Starting UT[a]	Airmass	Filter and Exposure time [b]	Standard Stars Fields
15:19	1.06	BVI: 30s; R: 15s	PG0918
15:30	1.14	BVI: 30s; R: 15s	SA104
15:39	1.06	B: 60s; VRI: 30s	GD108
15:51	1.26	B: 60s; VRI: 30s	PG1323
17:40	1.47	BVI: 30s; R: 15s	GD108
17:46	1.51	BVI: 30s; R: 15s	GD108
17:51	1.54	BVI: 30s; R: 15s	GD108
18:09	2.17	BVI: 60s; R: 30s	PG0918
18:30	1.05	B: 120s; V: 90s; RI: 30s	PG1323
18:42	1.07	BVRI: 30s	SA104
18:48	1.08	BVRI: 60s	SA104
18:58	1.06	BVRI: 60s	PG1323

[a] UT = Universal Time.

[b] Exposure time is in second. We reduced the exposure time in R-band because some standard stars were saturated if using the same exposure time as in V-band. Similarly, we increase the exposure time for some B-band images to increase the signal-to-noise ratio for the standard stars (as the Q.E. in B-band is generally lower than other longer wavelength bands).

The operating temperature of the CCD was set to -14^{o}C during our observations because of the high and varying ambient temperature around 30^{o}C. Therefore we employed the AUTODARK feature during the images acquisition. This feature will take a dark image with the same exposure time as the science image and subtracted from it, hence the dark current and the bias signal was immediately

removed from the science image. For flat-field images, we took a series of dome flat images in BVRI filters in day-time. A set of dark and bias frames was also taken at the same time to remove the bias and dark signals in the dome flat images.

3. Data Reduction and Analysis

The reduction of the CCD images was done within the IRAF (Image Reduction and Analysis Facility, available at http://iraf.noao.edu/) environment. We combined the dome flat images to create master flat images in each BVRI filters, after removed the bias and dark signals in each of the dome flat images, using the flat combine task in IRAF. Since the bias and dark signals have already been subtracted in our science images (see Section 2), we only applied the master flat images with ccdproc task to remove flat field signatures in the science images. We also performed the astrometric refinement on the reduced images using the solve-field code available from the astrometry.net package [8,9], with a tweak order of 2. Stars in the images will then have correct equatorial coordinates (Right Ascension α and Declination δ, in epoch of J2000) after the astrometric refinements.

3.1. Deriving the Transformation Equations

To determine the limiting magnitudes and night sky brightness at LNO, it is necessary to derive the conversion, or transformation, between the instrumental magnitudes and standard (or calibrated) magnitudes. Standard stars in our reduced images can be used for such purpose, as the standard magnitudes of them are available in [7]. We first extracted the instrumental magnitudes of the standard stars listed in Table 1 using the phot task in IRAF. Radius of the aperture was set to 5.93 pixels (or 7", see [7]). A larger annulus was used to estimate the background counts for each standard stars and subtracted from the aperture counts.

In preparing for solving the transformation equations, we performed the following steps. These include: (a) created a text file linking the reduced images and the standard stars found in the images; (b) executed the mknobsfile task on the text file from previous step and the output magnitude files from the phot task to prepare the necessary observation files (these observation files contain the information of BVRI instrumental magnitudes and air masses for each standard stars in the reduced images); (c) edited the fnlandolt.dat and tlandolt.dat files copied from the IRAF installation and executed the mkconfig task to create the configuration file; and (d) prepare a data file containing the standard magnitudes and colors taken from [7] for our standard stars. Once all the necessary input files were ready, we executed the fitparams task (with 2.5σ iterative outliers rejection) in IRAF to solve the following transformation equations in each BVRI filters: $m_{instr}=m_{std}+ZP+\zeta X+\eta C$, where m_{instr} & X are instrumental magnitudes and air masses based on observations, m_{std} & C are standard magnitudes and colors adopted from [7], and ZP, ζ & η represent the CCD zero-point, the air mass-term & the color-term, respectively, that need to be solved. Note that the ZP is relative to 25 mag (the initial setting given in IRAF's apphot package). Our solved transformation equations are presented below:

$$b = B + 4.512(\pm 0.030) + 0.476(\pm 0.022)X - 0.180(\pm 0.015)(B - V), \sigma = 0.043, \quad (1)$$

$$v = V + 4.286(\pm 0.018) + 0.363(\pm 0.013)X + 0.035(\pm 0.010)(B - V), \sigma = 0.030, \quad (2)$$

$$r = R + 4.046(\pm 0.010) + 0.292(\pm 0.006)X + 0.079(\pm 0.010)(V - R), \sigma = 0.016, \quad (3)$$

$$i = I + 4.555(\pm 0.010) + 0.232(\pm 0.007)X - 0.024(\pm 0.006)(V - I), \sigma = 0.017. \quad (4)$$

The lower case letters, *bvri*, represent the instrumental magnitudes, while the upper case letters, BVRI, are standard magnitudes (and colors) adopted from [7]. σ is the standard deviation from the fits. Instrumental magnitudes of the standard stars can be re-calibrated with equation (1) - (4) to standard magnitudes using the invertfit task in the IRAF's photcal package. Figure 1 compares the V-band magnitudes and colors for the standard stars after re-calibration and the standard values given in [7]. Good agreements can be seen from this Figure that illustrates the validity of our derived transformation equations.

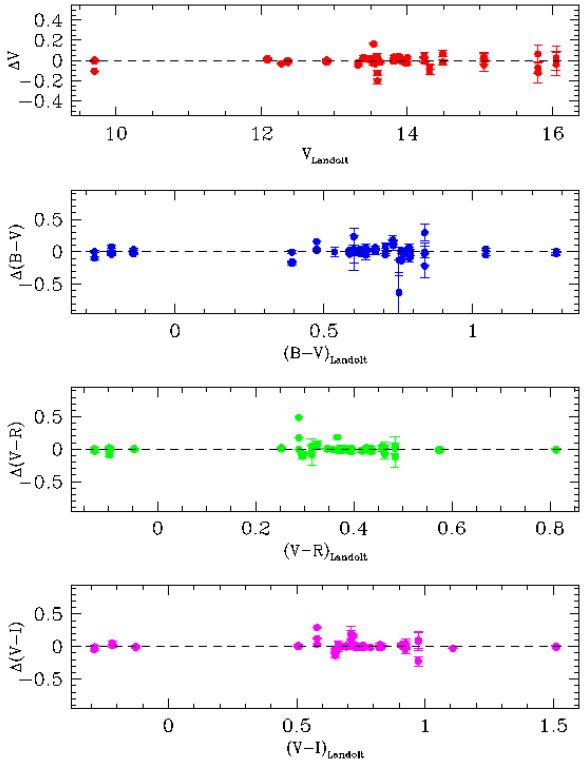

Figure 1. To evaluate the performance of our solved transformation equations, we compare the V-band magnitudes, the (B-V), (V-R) and (V-I) colors between our re-calibrated photometry, using equation (1) - (4), to the standard values taken from [7] as shown in the x-axes. The Δ in y-axes are the difference between them for the standard stars observed in this work. The dashed lines indicate Δ=0 and *not* the fit to the data. Results from this figure demonstrate that our solved transformation equations are reliable for a range of V-band magnitudes and colors.

3.2. Photometry for Stars in Standard Stars Fields

Stars located in our standard stars images, not just the standard stars, will be used to evaluate the limiting magnitudes at LNO. We first extracted the known stars or point sources that are expected to fall within our images from the 2MASS (The Two Micron All Sky Survey, [10]) All-Sky Point Source Catalog ([11]). The sky coordinates (α and δ in J2000) for these 2MASS sources were then converted to the pixel coordinates in (X,Y), using the wcs-rd2xy code from the astrometry.net package ([8,9]), and stored as coordinate files (.coo file). We also discarded 2MASS sources that located within 10 pixels from the edges of the images. With these coordinate files, aperture photometries were calculated with the phot task at the converted pixel locations of these 2MASS sources (a technique known as forced photometry), using a series of aperture sizes scaled with the seeing (or FWHM = Full-width at half maximum) of a given image. The later part is needed to calculate the aperture corrections using the mkapfile task. The calculated aperture corrections for each image was then applied to the aperture photometry based on an aperture radius of $3 \times FWHM$ of the images, and combined the BVRI photometry to a magnitude file with the mknobsfile task. Finally, these aperture-corrected instrumental magnitudes were calibrated to standard magnitudes using the results from previous sub-section by executing the invertfit task.

4. Estimation of Limiting Magnitudes and Night Sky Brightness at LNO

4.1. Estimating the Limiting Magnitudes

Limiting magnitudes from CCD images can be estimated using several methods (for examples, see [12,13]). In this work, we adopted the 5σ detection method demonstrated in [13]. This method is straight forward by plotting the magnitude errors versus the magnitudes, then the limiting magnitude at the 5σ detection level is the magnitudes where the magnitude error of 0.2 mag intersects with the data points in this plot. The BVRI-band calibrated magnitudes and their magnitude errors for the 2MASS sources in the standard stars images, based on the results from Section 3.2, were plotted in Figure 2(a), 2(b), 2(c) & 2(d). To find out the limiting magnitudes, we took an average of the calibrated magnitudes for those data points that have magnitude errors fall between 0.19 mag and 0.21 mag. Since images with 30 second and 60 second exposure time are common in all BVRI bands, we only determined the limiting magnitudes in these two sets of images. The estimated limiting magnitudes are presented in Table 2, where the errors represent the standard deviation of the means.

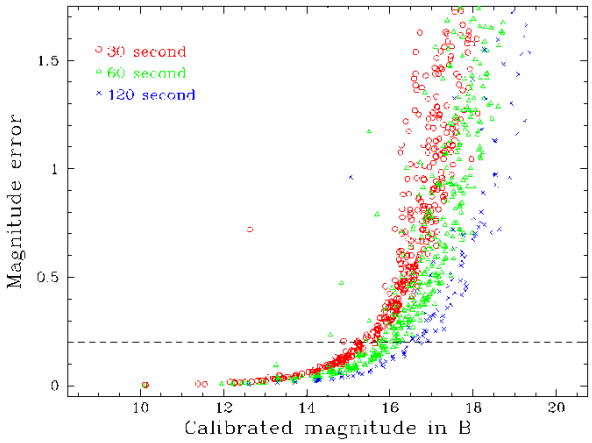

Figure 2(a). Plot of magnitude errors versus calibrated magnitudes in B-band for the 2MASS stars and point sources in our standard stars images. The horizontal dashed line indicates the magnitude error of 0.2 mag, corresponding to a signal-to-noise ratio of ~5.

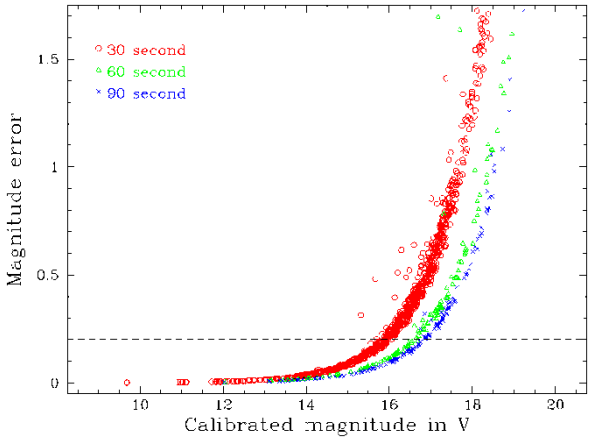

Figure 2(b). Plot of magnitude errors versus calibrated magnitudes in V-band for the 2MASS stars and point sources in our standard stars images. The horizontal dashed line indicates the magnitude error of 0.2 mag, corresponding to a signal-to-noise ratio of ~5.

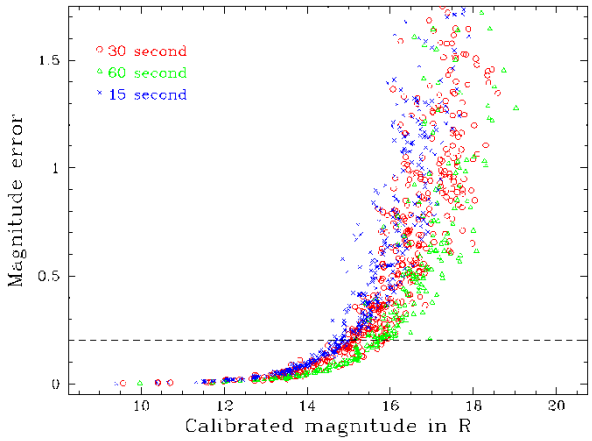

Figure 2(c). Plot of magnitude errors versus calibrated magnitudes in R-band for the 2MASS stars and point sources in our standard stars images. The horizontal dashed line indicates the magnitude error of 0.2 mag, corresponding to a signal-to-noise ratio of ~5.

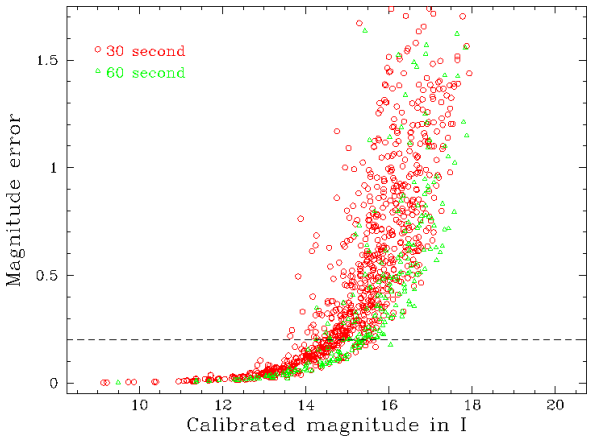

Figure 2(d). Plot of magnitude errors versus calibrated magnitudes in I-band for the 2MASS stars and point sources in our standard stars images. The horizontal dashed line indicates the magnitude error of 0.2 mag, corresponding to a signal-to-noise ratio of ~5.

Table 2. Estimated Limiting Magnitudes for the 5σ Detection at LNO.

Band	30 second exposure time [mag]	60 second exposure time [mag]
B	15.3±0.2	16.1±0.3
V	15.9±0.1	16.6±0.1
R	15.5±0.4	15.8±0.6
I	14.9±0.4	15.1±0.4

Our results revealed that the limiting magnitudes at LNO are ~15.4 mag and ~15.9 mag in exposure time of 30 and 60 second, respectively, regardless of the filters. Table 2 also shows that the best estimated limiting magnitude is in V-band, this is because the V-band data points in the magnitude errors versus magnitude plot do not exhibit large scatters as in other filters (see Figure 2). The larger scatters of data points seen in BRI bands are mainly due to the color terms, such as (B-V), (V-R) and (V-I), because magnitudes in these filters were calculated from the V-band magnitudes and colors. Therefore, uncertainties of the BRI-band magnitudes would be amplified and results a larger scatter toward fainter magnitudes. Because of this, we recommended using the V-band results (Table 2 and Figure 2) for the estimation of limiting magnitude when planning observations at LNO.

Figure 3 shows a small portion of the V-band image from one of our reduced standard stars images. On this Figure we also overlaid the locations of 2MASS sources with green circles, as well as labeled the calibrated V-band magnitudes on top of the circles. From this Figure we observed that sources brighter than ~17 mag are detectable, while sources with magnitudes between ~17 mag to ~18 mag are barely detected. The brightness of one source with V~20.6 mag in this Figure is almost same as the background noise. Hence, Figure 3 illustrates that our estimated limiting magnitudes are reliable.

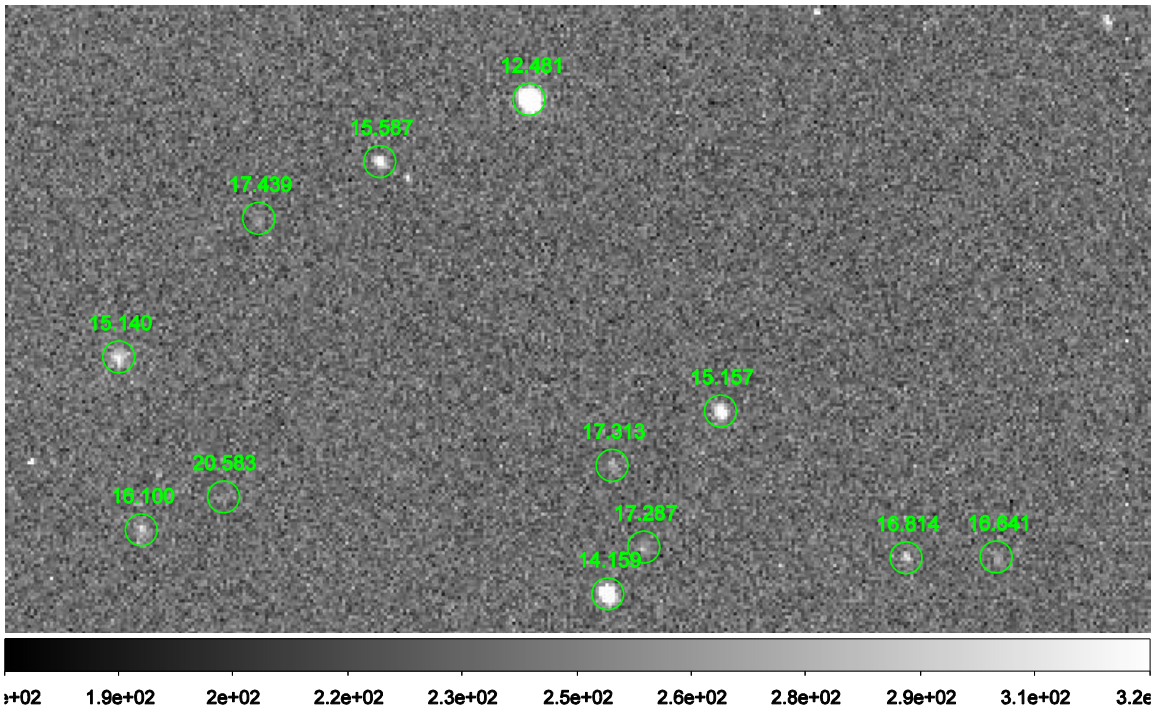

Figure 3. A small portion of one of the V-band image. Circles indicate the location of the 2MASS sources. The numbers above the circles are the calibrated V-band magnitudes for the given sources.

4.2. Estimating the Night Sky Brightness

Our standard stars images could also be used to estimate the night sky brightness at LNO. Since our images are relatively un-crowded, only a small fraction of the pixels will have high ADU counts due to illumination by stars light or cosmic rays. These high pixel values will be located at the (long) tail of the distribution (or histogram) for the count values of all pixels in an image, therefore the mode statistics (i.e. the peak of the distribution) is a good estimator of the night sky flux F_{sky} (expressed in ADU; on a single pixel) of the images. We employed the imstat task in IRAF to calculate the mode values or the F_{sky} for our standard star images. The instrumental night sky brightness is then expressed as (for examples, see [14,15]): $m_{sky}=Q-2.5\log(F_{sky}/A\ t_{exp})$, where Q=25.0 is the zero-point set in IRAF, t_{exp} is the exposure time (in second) of each images, and $A=1.44''^2$ is the area of a single pixel in the image. The unit of m_{sky} is mag arc-second^{-2}. We then calibrated these instrumental sky brightness to B_{sky}, V_{sky}, R_{sky} & I_{sky} using equation (1) - (4), assuming vanishing colors for the night sky.

Figure 4 shows the results of measured night sky brightness based on all of the standard stars images. The night sky brightness shows a clear trend that becoming brighter as air mass increases. Therefore, we fit a linear relation in the form of $M_{sky}=a+b(X-1)$ to the measurements shown in Figure 4, where M_{sky} represents the calibrated sky brightness in filter M. The measurements of night sky brightness are generally reported toward the zenith direction (for example, see [14] because usually it is the darkest part of the night sky. The intercepts of the linear relation, a, represent the night sky brightness at airmass of one (X=1), i.e. the zenith direction. Therefore, our final adopted night sky brightness at LNO is (measured at zenith): $B_{sky}=19.2\pm0.1$ mag arc-second^{-2}, $V_{sky}=19.0\pm0.1$ mag arc-second^{-2}, $R_{sky}=18.8\pm0.1$ mag arc-second^{-2} & $I_{sky}=18.1\pm0.1$ mag arc-second^{-2}. Our results in V- and R-band are consistent with the measurements made at the Weihai Observatory (WHO) of Shandong University ($V_{sky}^{WHO}\sim19.0$ mag~arc-second^{-2} & $R_{sky}^{WHO}\sim18.6$ mag arc-second^{-2} at the darkest night, [15].

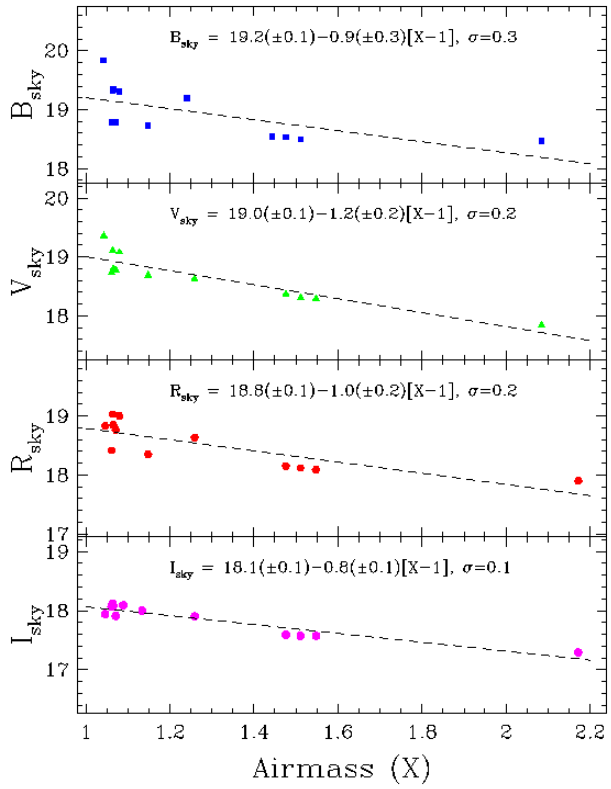

Figure 4. Based on our standard stars observations mentioned in Section 2, we measured the night sky brightness, in mag arc-second^{-2}, as a function of air mass in the BVRI bands. A trend is clearly seen from the data points such that the night sky brightness becomes brighter when air mass increases, therefore we fit a linear relation to the data points presented here. The dashed lines are fitted linear relation of the data points, with fitted results given at top of each panels. σ represents the dispersion of the linear fits. The night sky brightness in BVRI bands at zenith direction is represented by the intercepts of the fitted linear relations.

5. Conclusion

In this work, we measured the BVRI-band limiting magnitudes and night sky brightness at LNO. Our measurements were based on observations of selected standard stars fields taken on 01 April, 2016. This night represents typical observable nights at LNO, and hence our results can be used as guidance to plan the imaging observation at LNO with its 20-inch RC telescope. Our measured limiting magnitudes and night sky brightness were summarized in Table 2 and Figure 4, respectively. It is worth to point out that our results are not in disagreement with [6] – in fact both of the measurements on V-band night sky brightness are in good agreement. For the V-band limiting magnitudes, [6] inferred the limiting magnitude based on their sky brightness measurements using different telescope and instrument, while in our work we applied the 5σ detection method. Therefore, these different approaches could be the main reason behind a ~2 mag difference in the measured V-band limiting magnitudes.

Acknowledgments

This work was partly supported by the Taiwan's MOST grant 104-2112-M-008-012-MY3. We also thank the hospitality at LNO, especially the LNO staff Mohammad Redzuan Tahar and Karzaman Ahmad, during our stayed at the LNO. This publication makes use of data products from the Two Micron All Sky Survey, which is a joint project of the University of Massachusetts and the Infrared

Processing and Analysis Center/California Institute of Technology, funded by the National Aeronautics and Space Administration and the National Science Foundation. IRAF is distributed by the National Optical Astronomy Observatories, which are operated by the Association of Universities for Research in Astronomy, Inc., under cooperative agreement with the National Science Foundation.

References

[1] Szabo G M, Kiss L L, Benko J M *et al.* 2010 *Astronomy and Astrophysics* **523** A84
[2] Ahmad N and Zainuddin M Z 2009 *The Eighth Pacific Rim Conference on Stellar Astrophysics: A Tribute to Kam-Ching Leung* Astronomical Society of the Pacific Conference Series, vol 404, ed B Soonthornthum, S Komonjinda *et al.* (San Francisco: Astronomical Society of the Pacific) p 297
[3] Mohamad-Yob S-J, Gopir G K, Malasan H L and Anwar R 2009 *The Eighth Pacific Rim Conference on Stellar Astrophysics: A Tribute to Kam-Ching Leung* Astronomical Society of the Pacific Conference Series, vol 404, ed B Soonthornthum, S Komonjinda *et al.* (San Francisco: Astronomical Society of the Pacific) p 316
[4] Zainuddin M Z, Muhyidin M A, Ahmad N *et al.* 2011 *AIP Conference Proceedings* **1328** 56
[5] Loon C W, Zainuddin M Z, Ahmad N *et al.* 2015 *AIP Conference Proceedings* **1657** 050006
[6] Zainuddin M Z, Loon C W and Harun S 2010 *American Institute of Physics Conference Series* **1250** 51
[7] Landolt A U 2009 *The Astronomical Journal* **137** 4186
[8] Lang D, Hogg D W, Mierle K, Blanton M and Roweis S 2010 *The Astronomical Journal* **139** 1782
[9] Lang D, Hogg D W, Mierle K, Blanton M and Roweis S 2012 *Astrophysics Source Code Library* ascl:1208.001
[10] Skrutskie M F, Cutri R M, Stiening R *et al.* 2006 *The Astronomical Journal* **131** 1163
[11] Cutri R M, Skrutskie M F, van Dyk S *et al.* 2003 *VzieR On-line Data Catalog: II/246*
[12] Harris W E 1990 *Publications of the Astronomical Society of Pacific* **102** 949
[13] Gwyn S D J 2008 *Publications of the Astronomical Society of Pacific* **120** 212
[14] Duriscoe D M, Luginbuhl C B and Moore C A 2007 *Publications of the Astronomical Society of Pacific* **119** 192
[15] Guo D- F, Hu S- M, Chen X, Gao D- Y and Du J- J 2014 *Publications of the Astronomical Society of Pacific* **126** 496